UNSTRUCTURED 20-NODE BRICK ELEMENT MESHING

Guido D. Dhondt[1]

[1]MTU, Postfach 50 06 40, D-80976 Muenchen, Germany, guido.dhondt@muc.mtu.dasa.de

ABSTRACT

A new method is presented to generate an unstructured 20-node brick element mesh for arbitrary structures. Based on a triangulation of the structure's surface, a 20-node master mesh is generated encompassing the structure. The elements intersected by the triangulation are determined, catalogued, cut and remeshed according to their cutting topology. The new elements external to the structure are discarded, while the others are tied to the uncut subsurface mesh by means of multiple point constraints (MPC's). Alternatively, the remeshing procedure can be continued into the subsurface element layers to obtain a pure 20-node brick element mesh, without any MPC's. Additional smoothing further improves the mesh quality.

Keywords: automatic, hexahedral, mesh generation, cutting, smoothing, quadratic.

1. INTRODUCTION

Due to the availability of cheap computing power, three-dimensional analyses of complex structures are standard. However, the generation of a suitable mesh is still a formidable task, especially if hexahedral elements are preferred. Thus, compared to the computational time, the effort needed to generate the mesh generally dominates the overall process time. In the past, several proposals have been made to simplify the meshing job, ranging from modular building blocks [1] to finite octree techniques [2], midpoint division [3] and mesh projection near the free boundary [4]. An overview of these different techniques is given by the Handbook of Grid Generation [5]. However, the ultimate goal of a fully automatic tool to create a purely hexahedral mesh containing a reasonable number of elements for an arbitrary structure is still way off.

Here, a new technique is presented based on a cutting procedure originally developed for automatic crack propagation calculations [6][7]. The idea is to encompass the structure by a simple 20-node brick element mesh, the so-called master mesh, and to cut away all element parts not belonging to the structure. To this end, the structure's surface, which does not have to be connected, is described by a triangulation to be provided by the user. Based on this triangulation, the master mesh is generated in an automatic way. Then, all elements cut by the triangulation are determined and catalogued according to their cutting topology. Complex topologies are reduced to a set of seven simple topologies, for which a standard remeshing scheme is available. After remeshing, the new elements external to the structure are removed and a 20-node brick element mesh remains. However, since only the intersected elements were remeshed, there is a mesh density jump between the surface and subsurface elements in the structure. This jump can be taken care of by the use of multiple point constraints (MPC's), or, if the user prefers a pure 20-node brick element mesh, by continuing the remeshing into the deeper mesh layers until exhaustion. Then, a 20-node brick element mesh without any MPC's remains. The quality of the mesh can be further improved by smoothing. The use of 20-node brick elements has its origin in fracture mechanics applications [6][7]. However, it is expected that the method might work equally well with 8-node brick elements.

2. SURFACE TRIANGULATION AND MASTER MESH GENERATION

In order to mesh a structure, a suitable description of its shape must be available. In the present procedure the internal and/or external surfaces of the body must be provided in triangulated form. This type of description was chosen because of its simplicity, its flexibility and ready availability. Indeed, nearly all finite element preprocessors have the capability to mesh an arbitrary surface by triangles. While triangulating the surface, care has to be taken to model the details of the structure with sufficient accuracy. Since the triangulation of the surface is the only input to the procedure, the final hexahedral mesh quality largely depends on the quality of the triangulation. Characteristics missed by the triangulation will be lacking in the hexahedral mesh too.

A first step in the meshing procedure constitutes a careful analysis of the triangulation in order to detect topological characteristics such as edges and vertices. Edges and vertices are important since they constitute the backbone of the structure, and they should be accurately modeled by the hexahedral mesh. They are stored in linked lists for further use.

Once the triangulation has been analyzed, the master mesh is generated in an automatic way. It basically consists of a structured 20-node brick element mesh with the element edges parallel to the three Cartesian coordinate axes. Alternatively, the user is free to provide his own master mesh. This can be advantageous in order to exploit certain characteristics of the structure such as the axisymmetry in predominantly axisymmetric structures. Or, the present procedure can be used to insert additional details such as holes into an existing 20-node brick mesh. In that case the existing mesh can be used as master mesh. Without user intervention, the element size of the master mesh depends on the mean triangle side length in the triangulation.

3. MASTER MESH MODIFICATION

Once the master mesh is generated, all its edges are catalogued according to whether they are cut by the triangulation or not. An edge of a 20-node brick element contains two end nodes and one middle node. If the intersection point on such an intersected edge lies very close to one of the end nodes, all elements having this edge in common will be likely to yield very long and narrow or maybe very small elements after cutting. Thus, a first step aims at an improvement of the cutting geometry by moving the nodes of the intersected edges in such a way that the intersection point lies closer to the geometric middle point along the edge.

Figure 1 shows how this mesh modification procedure works. Element edge p3-p4-p5 is cut by the triangulation in a point close to p3. The distances from the intersection point I to p3 and p5 are d1 and d2 respectively. The nodes are labeled such that $d1 \leq d2$. The quantity $d=(d1+d2)/2$ is the mean of d1 and d2. If $|d-d1|/d<0.2$, the intersection point is deemed close enough to the middle node and no modification is made. Else, the radii $R1=(d1+d)/2$ and $R2=(d2+d)/2$ are calculated for future use.

Whether p3 and p5 are really moved depends on the existence of suitable element sides p1-p2-p3 and p5-p6-p7. Focusing on p1-p2-p3, an element side is looked for which:

1. does not belong to the elements containing side p3-p4-p5.
2. makes an angle $\alpha \leq 60°$ with the extension of p3-p4-p5 (Figure 1).
3. is not cut twice or more by the triangulation.

If no suitable side p1-p2-p3 is found, node p3 is not moved. If more than one suitable side is found, the one with the smallest α is taken. If the search for p1 and p2 was successful, the distance d3 from p1 to the intersection point I is determined. If $R1>0.75*d3$, which can occur if element side p1-p2-p3 is much smaller than p3-p4-p5, node p3 is not moved. Finally, if p1-p2-p3 is not cut, R3 is determined by $R3=(d3+R1)/2$ and node p3 is moved to a position on p1-p2-p3 on a distance R1 from I, node p2 is moved on a distance R3 from I. On the other hand, if p1-p2-p3 is cut in the intersection point J (Figure 1), the distance d5 between the intersection points is calculated and R1 is replaced by $R1=\min(R1,0.50*d5)$. If $R1 \leq d1$, node p3 is not moved. Else, R3 is determined and nodes p2 and p3 are moved in the same way as for the uncut side. Mutatis mutandis, the same procedure applies to element side p5-p6-p7. Finally, all midside nodes not already moved belonging to any sides of which one of the end nodes was moved, are moved into the middle of their end nodes. The new position of p2, p3, p4, p5 and p6 is shown by the gray circles in Figure 1. Simple examples of the effect of the procedure are available in [6].

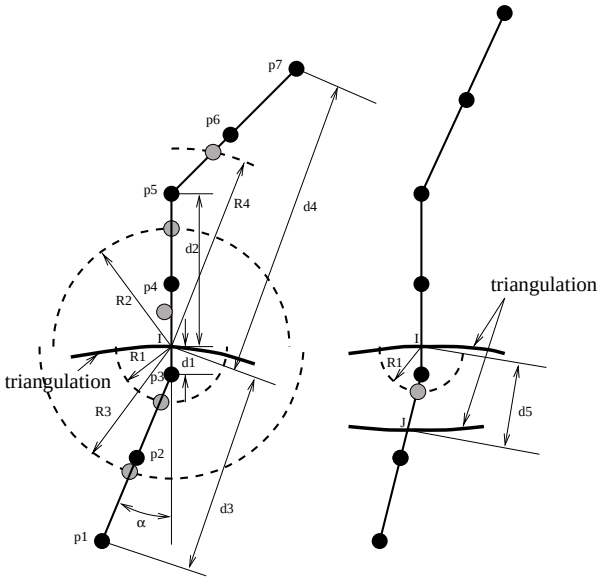

Figure 1. Mesh modification

4. SIMPLE AND COMPLEX TOPOLOGIES

After the mesh has been modified to improve the cutting geometry, all cut elements are catalogued according to the way in which they are cut. A distinction is made between simple and complex cutting topologies. A topology is simple if the following two conditions are satisfied:

1. each edge of the element is cut at most once by the triangulation,
2. the topology leads to at most two parts after cutting.

First, a check is performed whether any edge of the element at stake is cut more than once. If so, the element is replaced by newly generated elements having edges cut at most once, using a procedure discussed in the next section. In that stage, the topology belongs to one of the categories shown in Figure 2. To determine the category to which a specific element belongs, all vertex nodes of the element are labeled with 0 or 1, according to whether the node lies inside or outside the

structure. If there are more 1's than 0's the labels are reversed. The vertex nodes in Figure 2 with the black circles represent 1, the others 0. Thus, comparison with the schematic drawings in Figure 2 allows for a unique classification of the element at stake. The notation 1-7 in Figure 2 means that one corner node lies on one side of the triangulation, whereas all other seven nodes lie on the other side. The numbers in brackets show the number of variations for each scheme. For instance, for topology 1-7(a) there are eight ways in which to choose a corner node.

Figure 2 contains simple as well as complex topologies. Knowing that the element sides are cut at most once, a topology is simple if it leads to AT MOST two parts after cutting. This does not mean that a complex topology always leads to more than two parts. For instance, topology 2-6(b) can lead to two or three parts, depending on the actual triangulation. The fact that it CAN lead to more than two parts is sufficient to classify this topology as complex.

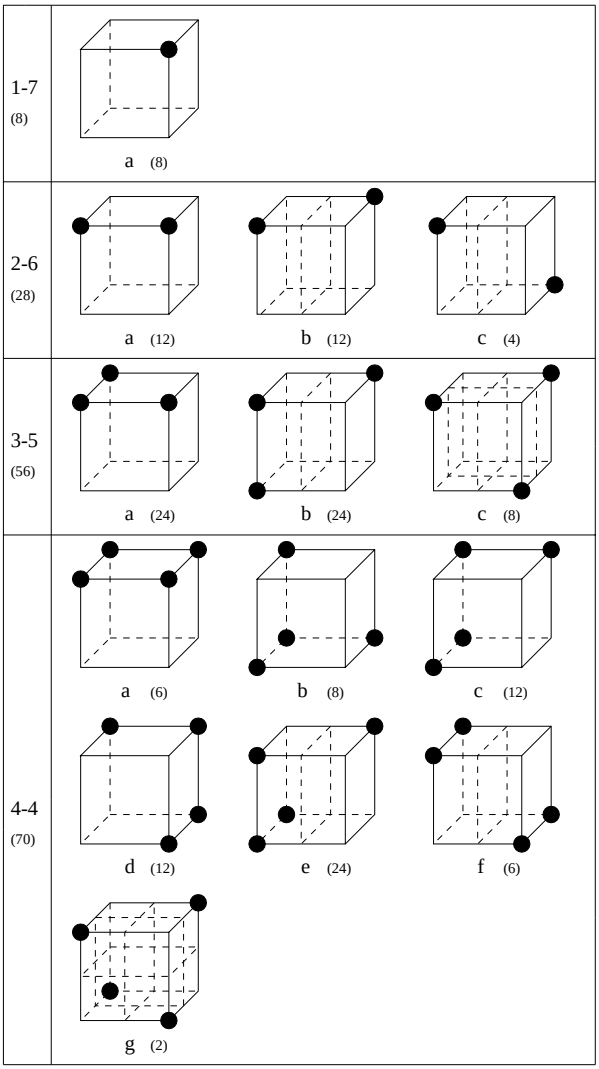

Figure 2. Classification of the single edge cut topologies

The only 1-7 topology is a simple one, 1-7(a). Cases 2-6 and 3-5 correspond each to one simple topology (a) and two complex topologies (b,c). Finally, case 4-4 corresponds to four simple and three complex topologies. Topology 4-4(d) is actually the mirror configuration of topology 4-4(c).

5. REDUCTION TO SIMPLE TOPOLOGIES

Once all intersected elements have been catalogued, the complex topologies are reduced to simple ones by cutting in between opposite element faces. This is performed in two steps. First, the elements with double cut edges are identified and cut in between the intersection points such that the newly generated elements have edges cut at most once. In the present implementation, edges cut more than twice are not covered. Although this can easily be changed, it might be advisable to use an overall finer master mesh in that situation.

Cutting by a plane in between two element faces generates two new elements which have to be connected with the surrounding elements. If the user wishes to avoid multiple point constraints, the cutting has to be pursued throughout the complete element layer until the free boundary of the master mesh is reached. This results in one element layer completely cut in two. On the other hand, if MPC's are allowed, the cutting of the layer can be stopped at elements which satisfy the following two conditions:

1. they contain no double cut edges
2. their edges which would be intersected by an extension of the cutting plane are not intersected by the triangulation.

This generally results in a subset of the element layer being cut in half and reduces the ultimate amount of elements.

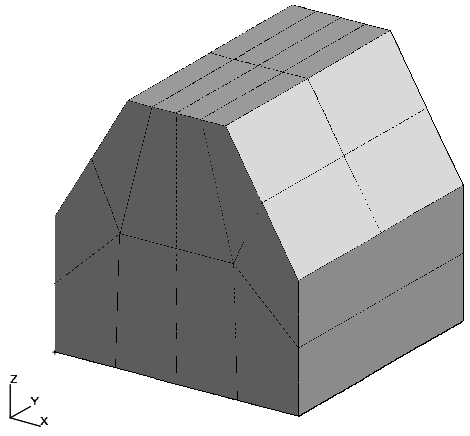

Figure 3. Element with double cut edges

Figure 3 shows an element in the form of a cube of which two wedge-like parts were removed by an appropriate triangulation. Before removal, two of the top edges were cut twice by the triangulation. The double cutting was reduced to simple cutting by dividing the element with a cutting plane parallel to the y-z plane. Then, the two new elements were remeshed and the wedges removed. Remeshing is treated in the next section.

Once all edges are cut at most once, all intersected elements belong to one of the topologies in Figure 2. The complex topologies are reduced to simple ones by introducing the cutting planes indicated by the dashed lines (Figure 2). In most cases a cutting in two new elements suffices. Topology 4-4(g), where eight new elements are generated, can actually also be reduced by cutting in four. However, a division in eight was preferred out of symmetry reasons. This configuration is very rare anyway.

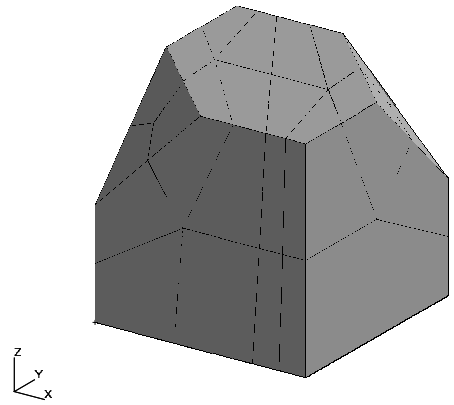

Figure 4. Reducing of complex topology 2-6(b)

An example of reducing complex topology 2-6(b) to two simple 1-7(a) topologies is given in Figure 4. Again, a subsequent remeshing and removal of external parts was performed after cutting.

6. CURVATURE, EDGE AND VERTEX PRESERVING REMESHING SCHEMES FOR THE SIMPLE TOPOLOGIES

At this stage, all intersected elements belong to simple topologies. For each of these topologies a remeshing scheme has been developed satisfying the following requirements:

1. only genuine 20-node brick elements are generated
2. compatibility between different topologies is assured
3. the curvature of the structure's surface, expressed by differently oriented triangles in the triangulation, can be adequately modeled
4. edges and vertices are accurately modeled.

The ensuing remeshing schemes are similar to the midpoint subdivision proposed by Li et al. [3]. However, the new nodes in the middle of the faces are generated using slightly different rules to improve the shape of the resulting elements. The remeshing for topology 3-5(a) is shown in Figures 5 and 6.

In all schemes only genuine 20-node brick elements are generated without recourse to tetrahedrons or other element types. All faces of the newly generated elements have four different nodes. Furthermore, by remeshing topologically identical faces of the master mesh element in exactly the same way, compatibility between different topologies is guaranteed.

So far, the triangulation was treated locally as a cutting plane. However, in reality, adjacent triangles are not necessarily coplanar and can model a curvature, an edge or a vertex. The curvature of the triangulation is taken into account by projecting the newly generated nodes within the cutting surface onto the triangulation.

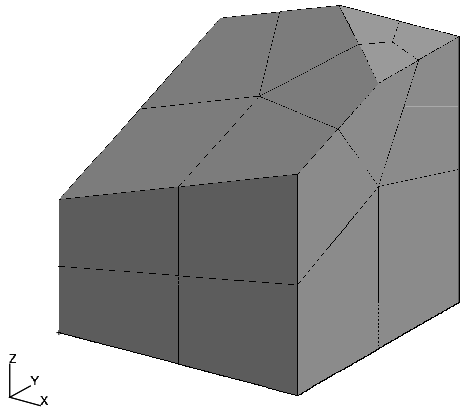

Figure 5. New mesh for topology 3-5(a) - part I

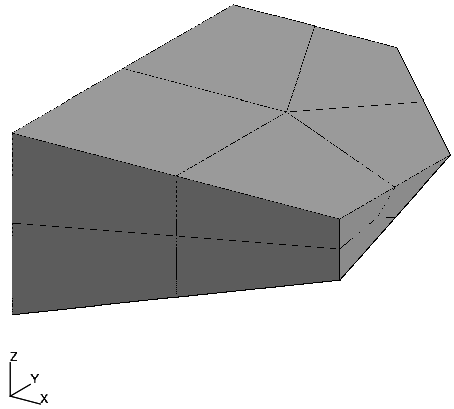

Figure 6. New mesh for topology 3-5(a) - part II

Modeling edges and vertices is more intricate. Looking at Figure 5, the slant cutting plane is remeshed using 5 element faces having one node in common. All nodes within the cutting plane can be freely used to provide an accurate picture of the triangulation. Thus, the node in the middle can be moved onto a vertex, if the triangulation contains such a vertex. Similarly, all nodes connected to this vertex node can be positioned exactly on edges in the triangulation. This is illustrated in Figure 7, where a sharp vertex was modeled using topology 1-7(a). All remeshing schemes are such, that

they can model exactly one sharp 3-dimensional vertex, if the need arises. The number of edges which may be attached to the vertex depends on the topology. For instance, topology 1-7(a) can accommodate 3 edges, whereas it is clear from Figure 5 that topology 3-5(a) can model 5 edges. More edges can be taken care of through additional cutting. The modeling of multiple vertices within one and the same master mesh element is to be handled by choosing a finer master mesh.

The situation for edges is similar. Each remeshing scheme can model at most one edge not containing a vertex within the element, or as many edges coinciding in a vertex as there are element faces within the cutting plane. However, multiple edges can be accounted for by additional cutting. This is generally necessary for two close (nearly) parallel edges, as is the case at the free borders of plates or shells. This additional cutting can be done after reduction to simple topologies and before remeshing.

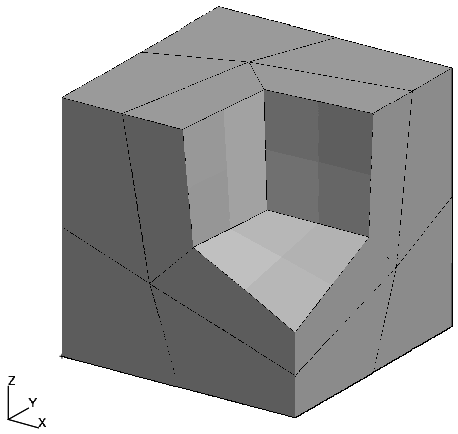

Figure 7. Modeling a vertex

7. A POSTERIORI MODIFICATIONS

After remeshing of the simple topologies, the resulting mesh consists of original master mesh elements external and internal to the structure, reduced master mesh elements external and internal to the structure and remeshed master mesh elements (possibly after reduction) internal and external to the structure. Now, all elements external to the structure are discarded. Then, a thin layer of fine remeshed elements close to the triangulation remains, covering original and reduced (but not remeshed) coarse master mesh elements. The connection between both is usually done by means of multiple point constraints. Due to remeshing, the uncut faces of a remeshed element are divided into four new element faces. For instance, this applies to the back faces of Figure 7. These four faces are tied by means of MPC's to the one underlying master mesh face.

Alternatively, if the user wishes to avoid MPC's, the remeshing can be continued into the structure by dividing each underlying master mesh element into eight parts. Ultimately, a MPC-less mesh is obtained by continuing this procedure until exhaustion. This, of course, increases the number of elements in the final mesh. However, since peak stresses usually occur at the surface of the structure, a couple of additional layers is usually sufficient.

Thus, a 20-node element mesh has been created for the structure at hand. Further improvement can eventually be obtained by smoothing the mesh. Smoothing existing meshes is really a field of its own. Here, merely two methods are presented aiming at satisfying two totally different criteria.

The first smoothing procedure aims at improving the Jacobian determinant in the integration points of the mesh. A negative Jacobian determinant points to negative volumes and leads to a crash of every finite element code. Thus, a procedure is started which identifies such integration points, and moves the corner nodes of the elements concerned while maximizing the Jacobian determinant in the element and its neighbors. The middle nodes of the elements are kept within a reasonable distance from the geometric middle point. The optimization algorithms used are very robust and based on the Nelder-Mead method [8]. Experience has shown that the method is very effective, but does not necessarily lead to visually pleasing meshes.

The second method uses a weighted Laplace smoothing procedure as described by Blacker and Stephenson [9]. Here, the nodes in the mesh are moved depending on the position of their neighbors. Examples of its application are shown in [7]. It leads to visually improved meshes, but does not guarantee the positiveness of the Jacobian determinant. It looks as if a combination of both smoothing procedures might yield an optimum technique. However, further research is needed.

8. EXAMPLES

In this section, three examples are given highlighting the applicability and efficiency of the method.

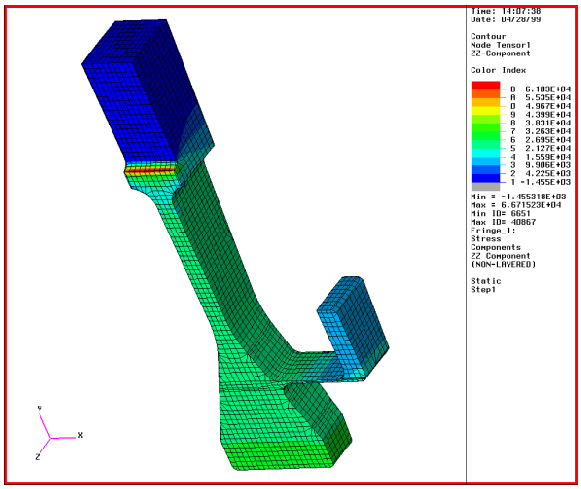

Figure 8. Turbine disk segment

The first example is a turbine disk segment (Fig 8). It is a predominantly axisymmetric structure with U-shaped notches in the rim area and a drive arm in between bore and rim. The

master mesh was a rectangular grid parallel to the Cartesian axes. If the disk segment were larger, an axisymmetric master mesh would probably be preferable. The size of the triangles in the triangulation was adapted to the local accuracy requirements.

Due to the small thickness of the drive arm, double cut edges arose. These were reduced to simple cut edges by intersecting the master mesh elements as explained in previous paragraphs. This led to a local refinement of the final mesh, as can be seen in Figure 8 and 10. Subsequently, the intersected elements were remeshed according to their topology and tied to the underlying master mesh elements using MPC's. No additional element layers were remeshed nor any Laplace smoothing performed. The final mesh contained 45139 nodes and 8731 elements. Figures 8, 9 and 10 show that the structure's details are accurately modeled: local curvature (note the small radii in the bore area), edges and vertices of the structure are well represented.

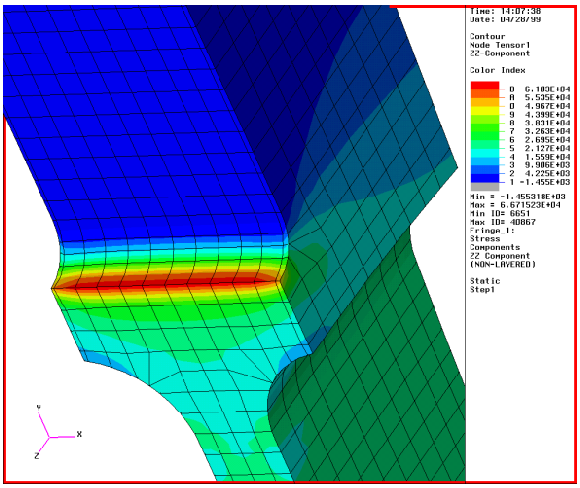

Figure 9. Detail of the rim area

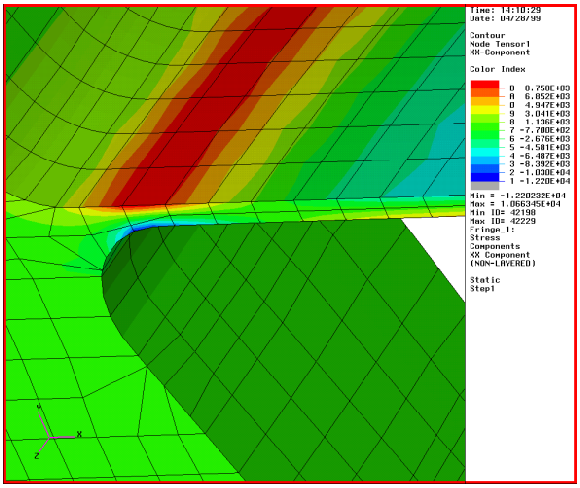

Figure 10. Detail of the drive arm construction

A stress calculation was performed under centrifugal loading. In figures 8 and 9 the hoop stress is plotted, in Figure 10 the axial stress is shown. The fringe plots are smooth and show the expected stress fields. At the bottom of the U-notch a hoop stress concentration arises with maximum value in the middle of the rim (Figure 9). In the drive arm bending stresses are generated involving tensile stresses at the top and compressive stresses at the bottom of the arm.

The second and third example are similar to two structures shown on a web site by Robert Schneiders [10].

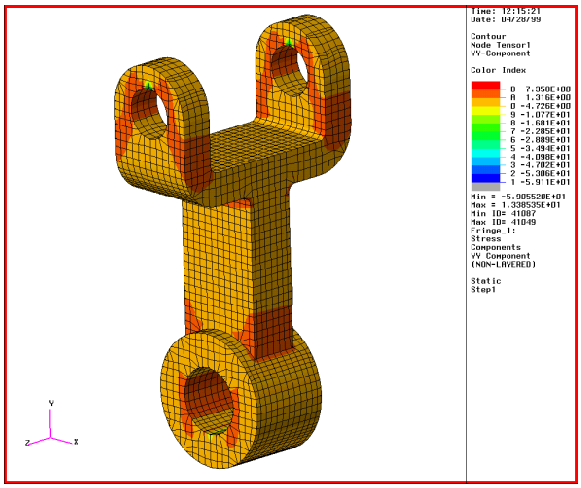

Figure 11. Structure with holes under tension

Example two is shown in Figure 11 and represents a connecting element between two axles. It is characterized by holes of different size and a relatively complex connection of the straight part and the lower hole.

The master mesh was generated automatically, and mesh modification was applied to improve the cutting topologies. All topologies were simple, so no additional cutting was necessary. Only the surface layer was remeshed and tied to the underlying structure using MPC's. No smoothing was applied. The final mesh contained 41408 nodes and 7986 elements.

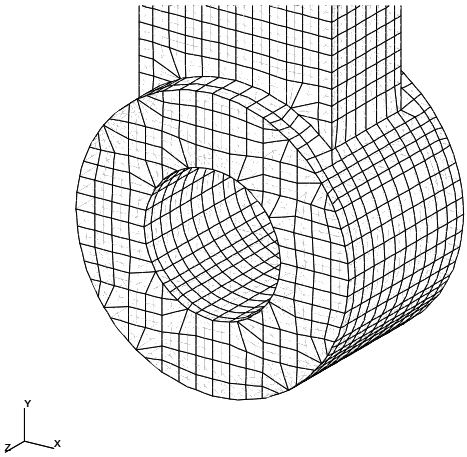

Figure 12. Detail of the lower ring

The overall mesh looks good. The curvature and edges of the

structure are well modeled. This also applies to the difficult connection of the straight part and lower ring (Figure 12). Additional Laplace smoothing could further improve the visual quality of the mesh.

Tensile forces were applied along the uppermost line within the upper rings, while the lowermost line in the lower ring was held fixed. The fringe plot in Figure 11 shows the normal stress in y-direction and looks very smooth. The usual stress concentrations near the loading points and fixed points arise. The local stress increase near the holes is also to be expected.

The last example (Figures 13, 14 and 15) is characterized by quite a few sharp edges and vertices. Here, a relatively fine master mesh was generated such that all topologies were simple. Again, the usual mesh modification was performed to improve the geometry of the intersected elements. Then, the intersected elements were catalogued according to their cutting topology and remeshed. One additional layer of elements was remeshed, pushing the MPC's one layer deeper. No additional smoothing was performed.

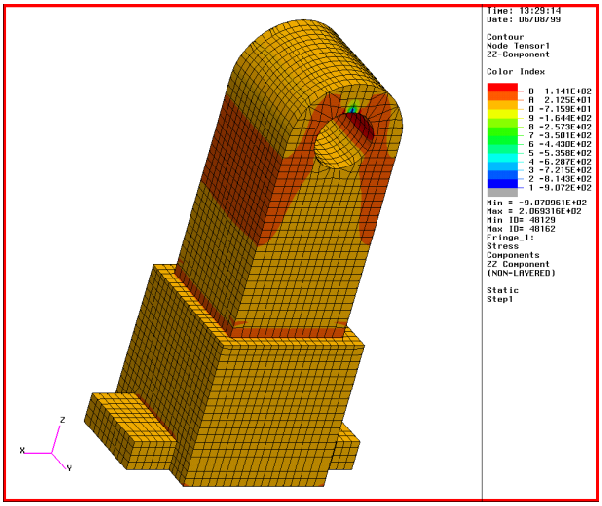

Figure 13. Stairs-like structure with hole

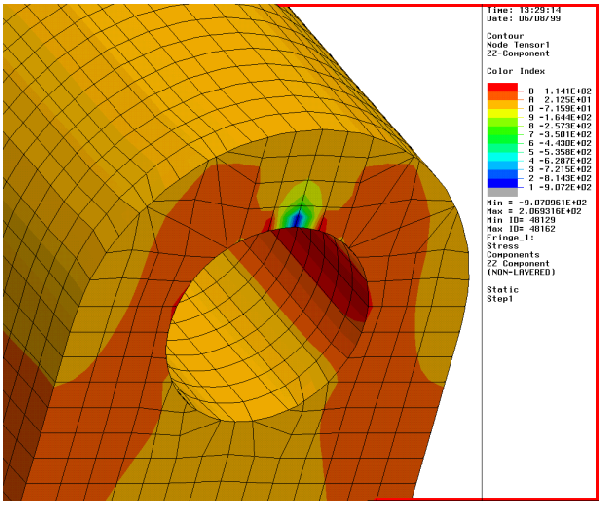

Figure 14. Detail of the hole

The resulting mesh is shown in Figure 13. The edges and vertices are well modeled, and so is the hole at the top of the structure. Due to the fine size of the master mesh, the final mesh contained 65538 nodes and 14128 elements. A stress calculation was performed for tensile forces in z-direction applied to the hole while the bottom plane was completely fixed. Figures 13 and 14 show the normal stress in z-direction. Concentrated compressive stress occurs at the location of the force application, while increased tensile stresses are observed around the hole and at geometric discontinuities. The elements in Figure 14 having dihedral angles greater than pi could be further removed using the method of "pillowing doublets" in [11].

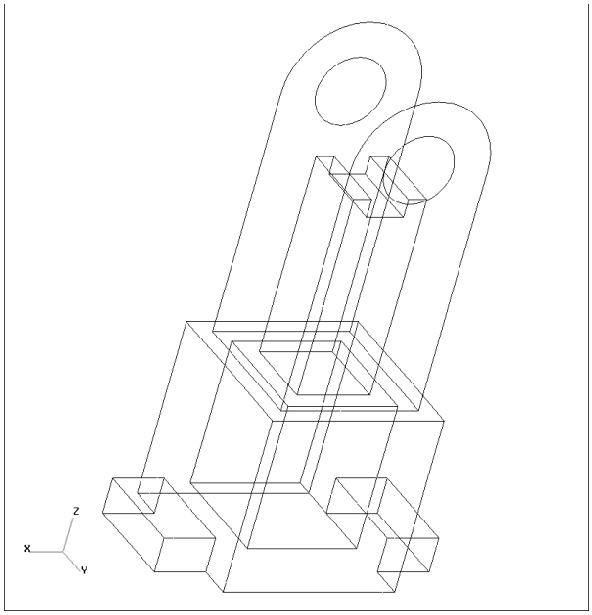

Figure 15. Internal and external edges

Figure 15 shows the external edges and vertices of the structure as detected by a finite element post-processing tool. They correspond exactly to the edges and vertices detected by the automatic meshing program based on the triangulation. In addition, Figure 15 also shows INTERNAL edges and vertices. These correspond to the transition of the fine remeshed zone to the underlying original master mesh zone. This is the interface where the MPC's are applied. By additional remeshing this interface might be further pushed inwards. However, the stress field pictures show that there is really no need for additional remeshing. The computational time for this linear elastic stress calculation on an state-of-the-art SGI workstation was about 1500 seconds. Starting from a coarser master mesh can further reduce this CPU-time.

9. CONCLUSIONS

A new method was presented to generate 20-node brick element meshes for arbitrary structures in a fully automatic way. The method excels due to its relative simplicity, its automatic execution, its ability to generate pure 20-node brick element meshes and the control over the depth of the remeshing procedure. Several examples have shown the

efficiency of the method.

REFERENCES

[1] S. Pissanetzky, "KUBIK: an automatic three-dimensional finite element mesh generator", *Int.J. Numer. Meth. Engng*, Vol 17 pp. 255-269 (1981)

[2] M.S. Shephard and M.K. Georges, "Automatic three-dimensional mesh generation by the finite octree technique", *Int. J. Numer. Meth. Engng*, Vol. 32 pp. 709-749 (1991)

[3] T.S. Li, R.M. McKeag and C.G. Armstrong, "Hexahedral meshing using midpoint subdivision and integer programming", *Comput. Mechods Appl. Mech. Engrg.*, Vol 124 pp. 171-193 (1995)

[4] R. Schneiders, "A grid-based algorithm for the generation of hexahedral element meshes", *Engineering with Computers*, Vol 12 pp. 168-177 (1996)

[5] J.F. Thompson, B.K. Soni and N.P. Weatherill (editors), "Handbook of grid generation", CRC Press London, 1998

[6] G. Dhondt, "Automatic 3-D Mode I crack propagation calculations with finite elements", *Int. J. Numer. Meth. Engng.*, Vol 41 pp. 739-757 (1998)

[7] G. Dhondt, "Cutting of a 3-D finite element mesh for automatic mode I crack propagation calculations", *Int. J. Numer. Meth. Engng.*, Vol 42 pp. 749-772 (1998)

[8] G.E. Gill, W. Murray and M.H. Wright, "Practical optimization", Academic Press, London (1981)

[9] T.D. Blacker and M.B. Stephenson, "Paving: a new approach to automated quadrilateral mesh generation", *J. Numer. Meth. Engng.,* Vol 32 pp. 811-847 (1991)

[10] R. Schneiders, "Mesh Generation & Grid Generation on the Web", www-users.informatik.rwth-aachen.de/~roberts/new_examples.html.

[11] T.J. Tautges, T. Blacker and S.A. Mitchell, “The whisker weaving algorithm: a connectivity-based method for constructing all-hexahedral finite element meshes”, *Int. J. Num. Meth. Engng.*, Vol 39 pp. 3327-3349 (1996)